Dalton Transactions

ROYAL SOCIETY OF CHEMISTRY

COMMUNICATION

View Article Online
View Journal | View Issue

Cite this: *Dalton Trans.*, 2024, **53**, 9664

Received 8th March 2024,
Accepted 24th May 2024

DOI: 10.1039/d4dt00708e

rsc.li/dalton

First-row transition metal carbonates catalyze the electrochemical oxygen evolution reaction: iron is master of them all†

Iranna Udachyan, [a] Jayesh T. Bhanushali, [a] Tomer Zidki, [a] Amir Mizrahi[b] and Dan Meyerstein*[a,c]

In pursuing green hydrogen fuel, electrochemical water-splitting emerges as the optimal method. A critical challenge in advancing this process is identifying a cost-effective electrocatalyst for oxygen evolution on the anode. Recent research has demonstrated the efficacy of first-row transition metal carbonates as catalysts for various oxidation reactions. In this study, Earth-abundant first-row transition metal carbonates were electrodeposited onto nickel foam (NF) electrodes and evaluated for their performance in the oxygen evolution reaction. The investigation compares the activity of these carbonates on NF electrodes against bare NF electrodes. Notably, $Fe_2(CO_3)_3$/NF exhibited superior oxygen evolution activity, characterized by low overpotential values, *i.e.* Iron is master of them all (R. Kipling, Cold Iron, Rewards and Fairies, Macmillan and Co. Ltd., 1910). Comprehensive catalytic stability and durability tests also indicate that these transition metal carbonates maintain stable activity, positioning them as durable and efficient electrocatalysts for the oxygen evolution reaction.

Introduction

The escalating global energy demand, driven by the surge in population, necessitates sustainable solutions, prominently exemplified by the utilization of renewable energy sources such as electrochemical water splitting.[1,2] Electrochemically generated hydrogen holds a distinct advantage in its ease of storage compared to other renewable sources, including solar, wind, and hydropower.[2,3] Furthermore, hydrogen emerges as a superior alternative to nonrenewable energy sources, offering a clean and green energy generation pathway. In the electrochemical water-splitting process, hydrogen evolution at the cathode is coupled with oxygen evolution at the anode.[4,5] The sluggish kinetics of the latter process, involving a four-electron transfer, presents a bottleneck.[6]

To date, noble metal oxides, notably IrO_2 and RuO_2, have been recognized for their efficiency as catalysts for the oxygen evolution reaction (OER). However, their commercial viability is hindered by the prohibitive cost and limited availability of noble metals.[7,8] Consequently, substantial efforts are underway to design catalysts with advanced materials using Earth-abundant transition metals.[9–12]

Recent studies have identified first-row transition metal carbonates as promising catalysts for electrochemical oxidation processes.[13–22] These metal carbonates, widely employed in industrial applications such as plastics, paper, paint, and rubber industries, have shown utility in various electrochemical catalytic reactions.[23–26] Metal carbonates are widely used in solid oxide fuel cells, batteries, and supercapacitors.[27–29] Notably, the carbonate's role as σ-donor ligand stabilizes high oxidation states of metals like Mn^{III}, $Fe^{IV/III}$, $Co^{V/IV/III}$, Ni^{III}, and $Cu^{IV/III}$, facilitating the stabilization of metal complexes' high oxidation states and partial radicalization of the carbonate ligand.[16,17,30–32] In the high oxidation states of these complexes, the carbonate functions as an electron donor to the central metal cation, stabilizing the high oxidation states of metal complexes while also inducing partial radicalization of the carbonate ligand.[18,19] Additionally, metal complex intermediates in higher oxidation states boost electrochemical reactions.

The report by Chen *et al.* shows that incorporating Fe in NiFeOx catalysts enhances the water oxidation activity and delivers a stable current density of 100 mA cm^{-2} in an alkaline media.[31] Building on this background, the present study demonstrates a series of first-row transition metal carbonates as effective OER catalysts and identifies the most potent catalyst among them. Electrochemical deposition of the metal carbonate complexes onto Ni foam substrate (NF) was accomplished through anodization in aqueous electrolytes. The synthesized catalysts were comprehensively analyzed for their chemical and physical properties through various spectro-

[a]*Department of Chemical Sciences, and The Radical Research Center, Ariel University, Ariel, Israel. E-mail: danm@ariel.ac.il*
[b]*Chemistry Department, Nuclear Research Centre Negev, Beer-Sheva 8419001, Israel*
[c]*Department of Chemistry, Ben-Gurion University, Beer-Sheva, Israel*
† Electronic supplementary information (ESI) available. See DOI: https://doi.org/10.1039/d4dt00708e

scopic techniques. Subsequently, the activity of the deposited metal carbonate complexes on the NF electrode in the electrochemical OER was determined and compared.

The experimental procedures for the electrochemical deposition of metal carbonates, their respective characterization, and electrochemical activity are described in the ESI.†

Results and discussion

All metal carbonates were deposited electrochemically on the NF surface using the standard three-electrode cell setup by chronoamperometry at 1.1 V *vs.* Ag/AgCl. The electrochemically deposited metal carbonates on the NF surface were subjected to various physical and chemical characterization tools. Firstly, all the metal carbonates on NF and bare NF were subjected to FE-SEM analysis to determine the morphology and particle sizes. The results obtained are presented in Fig. 1. From Fig. 1a, NF exhibited a smooth surface. $Mn_2(CO_3)_3$/NF showed a random orientation of spherical particles on NF to form a cauliflower-like morphology.[33] Similarly, $Fe_2(CO_3)_3$/NF, $Co_2(CO_3)_3$/NF, $Ni_2(CO_3)_3$/NF, and $Cu(CO_3)$/NF also displayed spherical morphologies with randomly orientated microspheres. Moreover, specific flakes of carbonate species were clearly observable in $Cu(CO_3)$/NF.

The interaction type between the metal and carbonate was explored by ATR-IR spectroscopy. The IR spectrum of $Mn_2(CO_3)_3$/NF is presented in Fig. 2a. The peak at 1713 cm^{-1} is ascribed to CO stretching. Further, 1410, 864, and 718 cm^{-1} peaks are characteristic $Mn_2(CO_3)_3$ peaks,[34] corresponding to asymmetric stretching of CO_3^{2-}, out-of-plane, and in-plane bending vibrations, respectively.[35,36] Similarly, the other metal carbonates showed similar IR spectra, which are presented in the ESI (Fig. S1†).

XPS analysis of the metal carbonates on the NF electrode was performed to determine the elemental composition and their oxidation states. The obtained XPS spectra are presented in Fig. 2b–d. $Fe_2(CO_3)_3$/NF showed the presence of Fe in +2 and +3 oxidation states, as noted from the Fe $2p_{3/2}$ (712.1 eV) and Fe $2p_{1/2}$ (725.0 eV) peaks and their respective satellite peaks (714.9 and 727.8 eV) (Fig. 2b).[37] Similarly, $Ni_2(CO_3)_3$/NF and $Cu(CO_3)$/NF displayed the presence of Ni in +2, +3 oxidation states (Fig. 2c)[38] and Cu in +2 oxidation state (Fig. 2d)[39] by the Ni $2p_{3/2}$ (855.4 eV), Ni $2p_{1/2}$ (873.3 eV), Cu $2p_{3/2}$ (934.9 eV), and Cu $2p_{1/2}$ (954.6) peaks along with their respective satellite peaks (Ni $2p_{3/2}$ 861.8 eV, Ni $2p_{1/2}$ 879.2 eV, Cu $2p_{3/2}$ 943.4 eV and Cu $2p_{1/2}$ 962.7). The data corresponding to other metal carbonates, namely, $Co_2(CO_3)_3$/NF and $Mn_2(CO_3)_3$/NF, are presented in Fig. S2.† In addition, carbon and oxygen signals were detected in the XPS analysis of the metal carbonates, as seen in Fig. S2f–j.†

The electrochemically deposited $Mn_2(CO_3)_3$/NF, $Fe_2(CO_3)_3$/NF, $Co_2(CO_3)_3$/NF, $Ni_2(CO_3)_3$/NF, and $Cu(CO_3)$/NF were investigated for the oxygen evolution reaction in 1.0 M KOH N_2-purged solutions using the standard three-electrode system with a scan rate of 20 mV s^{-1}. Fig. 3a shows the LSV curves (without IR correction) for $Mn_2(CO_3)_3$/NF, $Fe_2(CO_3)_3$/NF, $Co_2(CO_3)_3$/NF, $Ni_2(CO_3)_3$/NF, $Cu(CO_3)$/NF, CO_3/NF, and NF. To

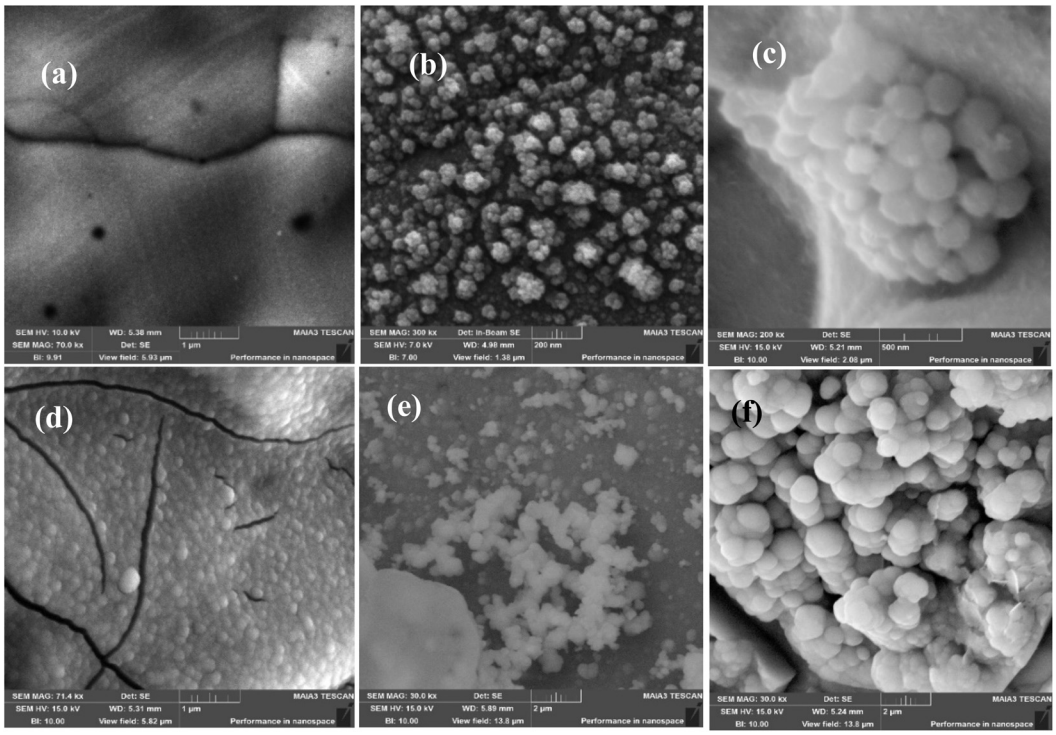

Fig. 1 SEM images of NF (a), $Mn_2(CO_3)_3$/NF (b), $Fe_2(CO_3)_3$/NF (c), $Co_2(CO_3)_3$/NF (d), $Ni_2(CO_3)_3$/NF (e), $Cu(CO_3)$/NF (f).

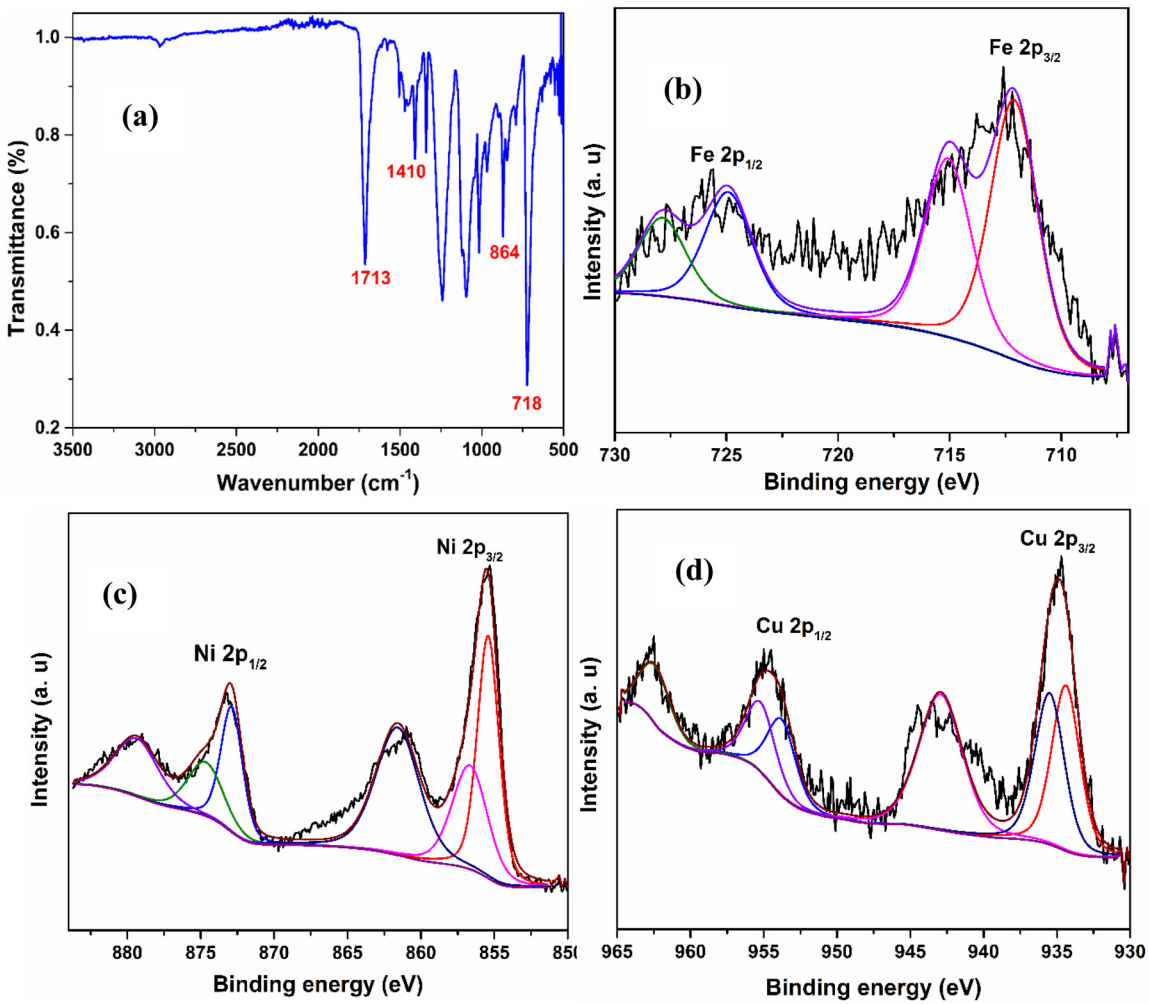

Fig. 2 ATR spectrum of $Mn_2(CO_3)_3$ (a), XPS spectra of Fe 2p for $Fe_2(CO_3)_3$/NF (b), Ni 2p for $Ni_2(CO_3)_3$/NF (c) and Cu 2p for $Cu(CO_3)$/NF (d).

begin with, the highest electrocatalytic activity for oxygen evolution was observed for the $Fe_2(CO_3)_3$/NF electrode with 10 mA cm^{-2} current density at a low overpotential of 310 mV (1.54 V *vs.* RHE), which is much lower in comparison with the other metal carbonates. Also, the other catalysts achieved 10 mA cm^{-2} current densities at low over potential values namely, $Mn_2(CO_3)_3$/NF at 360 mV (1.59 V *vs.* RHE), $Co_2(CO_3)_3$/NF at 390 mV (1.62 V *vs.* RHE), $Ni_2(CO_3)_3$/NF at 350 mV (1.58 V *vs.* RHE), $Cu(CO_3)$/NF at 400 mV (1.63 V *vs.* RHE), CO_3/NF at 460 mV (1.69 V *vs.* RHE), and bare NF at 520 mV (1.75 V *vs.* RHE), respectively. These results indicate that first-row transition metal carbonates are active electrocatalysts for the OER. Among these metal carbonates, the $Fe_2(CO_3)_3$/NF showed superior electrocatalytic behavior with the lowest overpotential. Furthermore, all the metal carbonates show multiple oxidation peaks before the sharp catalytic current peak for water oxidation, as was observed from the respective cyclic voltammograms, Fig. 3b. Additional results obtained are explained in the ESI.† Moreover, a comparative study was performed between the metal carbonates and the substrates used for the deposition of these metal carbonates to determine the effect on the OER activity. The results thus obtained are presented in the ESI.†

Additionally, Tafel curves were used to study the kinetics of the OER; the data is provided in Fig. 3c. The corresponding Tafel slope curves were fitted with the Tafel equation ($\eta = b \log j + a$, η = overpotential, j = current density, b = Tafel slope).[40,41] From Fig. 3b, $Fe_2(CO_3)_3$/NF displayed the lowest Tafel slope of 86 mV dec^{-1} compared to the other metal carbonates. Correspondingly, $Mn_2(CO_3)_3$/NF, $Co_2(CO_3)_3$/NF, $Ni_2(CO_3)_3$/NF, $Cu(CO_3)$/NF, CO_3/NF, and NF displayed Tafel slopes of 106 mV dec^{-1}, 96 mV dec^{-1}, 110 mV dec^{-1}, 112 mV dec^{-1}, 112 mV dec^{-1} and 122 mV dec^{-1}, respectively. The results indicate that metal carbonates show rapid reaction kinetics for oxygen evolution.[42,43]

Moreover, the electron transfer kinetics for the OER were determined by electrochemical impedance spectroscopy (EIS). Fig. S4† shows the EIS-Nyquist plot of the metal carbonates. The experiments relating to EIS were carried out at constant potential for oxygen evolution, as mentioned in the caption of

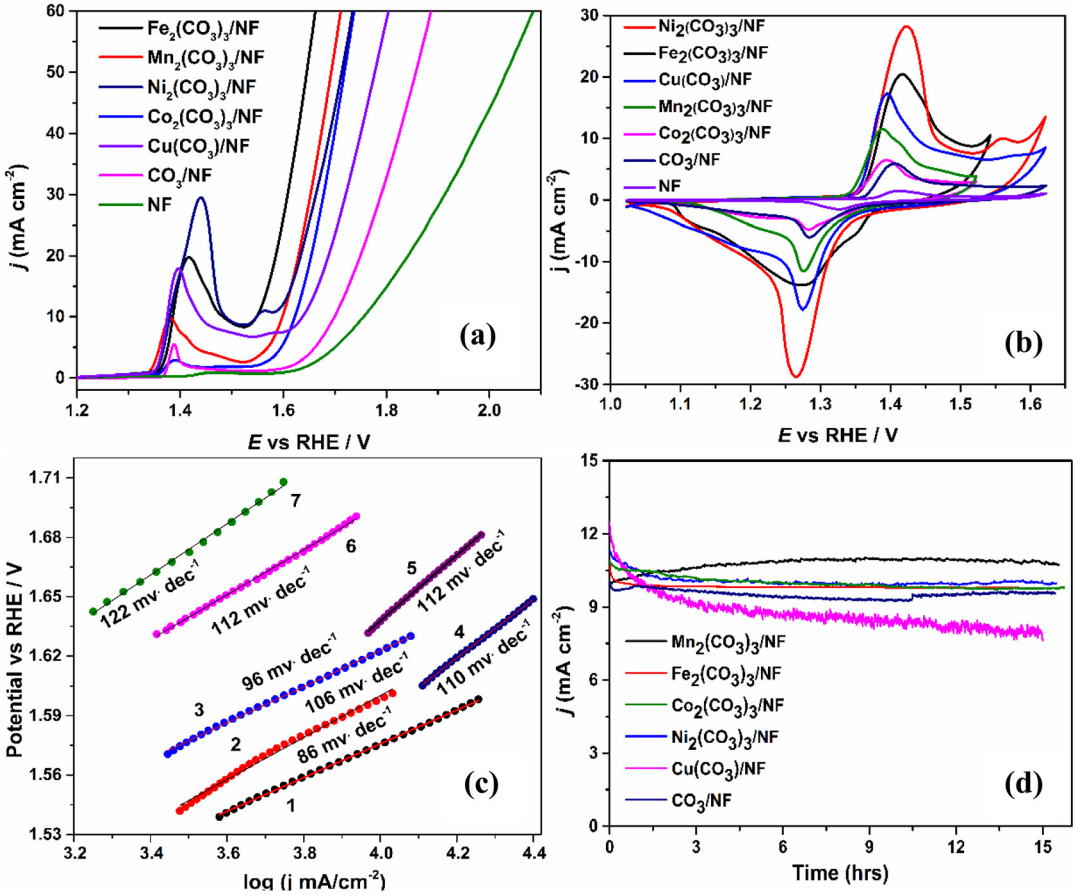

Fig. 3 Linear sweep voltammogram graphs at a scan rate of 20 mV s^{-1} in 1.0 M KOH (a), CV curves in 1.0 M KOH (b), the Tafel curves for $Fe_2(CO_3)_3$/NF, $Mn_2(CO_3)_3$/NF, $Co_2(CO_3)_3$/NF, $Ni_2(CO_3)_3$/NF, $Cu(CO_3)$/NF, CO_3/NF, and NF electrode in 1.0 M KOH (c) and long-term stability study of $Mn_2(CO_3)_3$/NF electrode at 1.59 V *vs.* RHE, $Fe_2(CO_3)_3$/NF electrode at 1.54 V *vs.* RHE, $Co_2(CO_3)_3$/NF electrode at 1.62 V *vs.* RHE, $Ni_2(CO_3)_3$/NF electrode at 1.58 V *vs.* RHE, $Cu(CO_3)$/NF electrode at 1.63 V *vs.* RHE and CO_3/NF electrode at 1.70 V *vs.* RHE in 1.0 M KOH (d).

Fig. S4.† All the metal carbonates exhibited smaller charge transfer resistance (R_{ct}) than NF and CO_3/NF. Interestingly, $Co_2(CO_3)_3$/NF showed a bit higher charge transfer resistance; the values are given in Table S1.† These metal carbonates may be considered suitable electron transfer catalysts and exhibit good conductivity towards electrochemical OER.[44–46]

Further, the key factor for a catalyst to be applied depends on its long-term stability and durability. Therefore, chronoamperometric analysis was carried out in 1.0 M KOH for the metal carbonates/NF with CO_3/NF to determine their stability for a duration of 15 h; the results are presented in Fig. 3d. $Mn_2(CO_3)_3$/NF, $Fe_2(CO_3)_3$/NF, $Co_2(CO_3)_3$/NF, $Ni_2(CO_3)_3$/NF and CO_3/NF showed good electrocatalytic stability whereas, $Cu(CO_3)$/NF showed decrement in electrocatalytic stability. The analysis was performed for all catalysts at their respective electrocatalytic oxygen evolution potentials. The results indicate no significant change in catalytic current density after 15 h except for a slight decay in the catalytic current density in the initial stage of the experiment for $Fe_2(CO_3)_3$/NF, $Co_2(CO_3)_3$/NF, $Ni_2(CO_3)_3$/NF and $Cu(CO_3)$/NF. After one h, the current density stabilized for $Fe_2(CO_3)_3$/NF, whereas $Cu(CO_3)$/NF exhibited slight decay in the catalytic current density throughout the analysis.

Conclusions

In summary, first-row transition metal carbonates were deposited by electrochemical deposition on a nickel foam (NF) electrode surface, and the electrodeposited metal carbonates were physically and chemically characterized using various characterization techniques. The electrochemically deposited metal carbonates with CO_3/NF were successfully used for the electrochemical oxygen evolution reaction. Additionally, $Mn_2(CO_3)_3$/NF, $Fe_2(CO_3)_3$/NF, $Co_2(CO_3)_3$/NF, $Ni_2(CO_3)_3$/NF, $Cu(CO_3)$/NF, CO_3/NF displayed overpotentials of 360 mV, 310 mV, 390 mV, 350 mV, 400 mV, 460 mV and 520 mV, respectively. Considering the overpotential values, the study clearly demonstrates that iron, the cheapest transition metal investigated for the OER, is the best catalyst. Tafel curves indicated lower slope value and faster electron transfer reaction followed by the EIS showing lower R_{ct} values, supporting the faster reaction kine-

tics. The long-term stability and catalytic durability test inferred that first-row transition metal carbonates are stable catalysts for electrochemical oxygen evolution. The plausible roles of transition metal carbonates as catalysts of OER were discussed in ref. 15.

Conflicts of interest

The authors declare that there are no conflicts of interest to declare.

Acknowledgements

The authors are indebted to the Pazy Foundation (Grant No. RA1700000176) for financial support, and I. U. is thankful to Ariel University for a Ph.D. Fellowship.

References

1 M. Amin, H. H. Shah, A. G. Fareed, W. U. Khan, E. Chung, A. Zia, Z. U. R. Farooqi and C. Lee, *Int. J. Hydrogen Energy*, 2022, **47**(77), 33112–33134.
2 S. Y. Tee, K. Y. Win, W. S. Teo, L. Koh, S. Liu, C. P. Teng and M. Han, *Adv. Sci.*, 2017, **4**, 1600337.
3 X. Li, X. Hao, A. Abudula and G. Guan, *J. Mater. Chem. A*, 2016, **4**, 11973–12000.
4 L. Li, P. Wang, Q. Shao and X. Huang, *Chem. Soc. Rev.*, 2020, **49**, 3072–3106.
5 J. Wang, W. Cui, Q. Liu, Z. Xing, A. M. Asiri and X. Sun, *Adv. Mater.*, 2016, **28**, 215–230.
6 K. Zhang and R. Zou, *Small*, 2021, **17**, 2100129.
7 Z. Tao, T. Wang, X. Wang, J. Zheng and X. Li, *ACS Appl. Mater. Interfaces*, 2016, **8**, 35390–35397.
8 Z. Wu, X. F. Lu, S. Zang and X. W. Lou, *Adv. Funct. Mater.*, 2020, **30**, 1910274.
9 Y. Zhang, J. Wu, B. Guo, H. Huo, S. Niu, S. Li and P. Xu, *Carbon Energy*, 2023, **5**, e375.
10 R. Liang, B. Zhang, Y. Du, X. Han, S. Li and P. Xu, *ACS Catal.*, 2023, **13**, 8821–8829.
11 B. Guo, Y. Ding, H. Huo, X. Wen, X. Ren, P. Xu and S. Li, *Nano-Micro Lett.*, 2023, **15**, 57.
12 J. Zhao, Y. Zhang, Y. Xia, B. Zhang, Y. Du, B. Song, H.-L. Wang, S. Li and P. Xu, *Appl. Catal., B*, 2023, **328**, 122447.
13 I. Udachyan, T. Zidki, A. Mizrahi, S. G. Patra and D. Meyerstein, *ACS Appl. Energy Mater.*, 2022, **5**, 12261–12271.
14 I. Udachyan, J. T. Bhanushali, A. Mizrahi, T. Zidki and D. Meyerstein, *ACS Appl. Energy Mater.*, 2022, **5**, 13903–13912.
15 S. G. Patra, A. Mizrahi and D. Meyerstein, *Acc. Chem. Res.*, 2020, **53**, 2189–2200.
16 A. Mizrahi, E. Maimon, H. Cohen, H. Kornweitz, I. Zilbermann and D. Meyerstein, *Chem. – Eur. J.*, 2018, **24**, 1088–1096.
17 A. Burg, Y. Wolfer, D. Shamir, H. Kornweitz, Y. Albo, E. Maimon and D. Meyerstein, *Dalton Trans.*, 2017, **46**, 10774–10779.
18 A. Mizrahi and D. Meyerstein, in *Adv. Inorg. Chem*, Elsevier, 2019, 74, 343–360.
19 S. G. Patra, E. Illés, A. Mizrahi and D. Meyerstein, *Chem. – Eur. J.*, 2020, **26**, 711–720.
20 J. Du, Z. Chen, S. Ye, B. J. Wiley and T. J. Meyer, *Angew. Chem., Int. Ed.*, 2015, **54**, 2073–2078.
21 T. Nishimoto, T. Shinagawa, T. Naito, K. Harada, M. Yoshida and K. Takanabe, *ChemSusChem*, 2023, **16**, e202201808.
22 M. Maazallahi, R. Bagheri, S. Nandy, K. H. Chae and M. M. Najafpour, *ACS Appl. Energy Mater.*, 2023, **6**(10), 5536–5547.
23 O. A. Jimoh, K. S. Ariffin, H. Hussin and A. E. Temitope, *Carbonates Evaporites*, 2018, **33**, 331–346.
24 S. Eloneva, S. Teir, J. Salminen, C.-J. Fogelholm and R. Zevenhoven, *Ind. Eng. Chem. Res.*, 2008, **47**, 7104–7111.
25 K. Song, in *Progress in Rubber Nanocomposites*, Elsevier, 2017, pp. 41–80.
26 F. C. Donnelly, F. Purcell-Milton, V. Framont, O. Cleary, P. W. Dunne and Y. K. Gun'ko, *Chem. Commun.*, 2017, **53**, 6657–6660.
27 L. Fan, C. He and B. Zhu, *Int. J. Energy Res.*, 2017, **41**, 465–481.
28 R. Zhang, Q. Fu, P. Gao, W. Zhou, H. Liu, C. Xu, J.-F. Wu, C. Tu and J. Liu, *J. Energy Chem.*, 2022, **70**, 95–120.
29 Y. Wang, C. Shi, Y. Chen, D. Li, G. Wu, C. Wang, L. Guo and J. Ma, *Electrochim. Acta*, 2020, **363**, 137236.
30 A. Khorobrykh, J. Dasgupta, D. R. J. Kolling, V. Terentyev, V. V. Klimov and G. C. Dismukes, *ChemBioChem*, 2013, **14**, 1725–1731.
31 J. Wang, L. Ji and Z. Chen, *ACS Catal.*, 2016, **6**, 6987–6992.
32 Z. Zhao, Z. Wang, D. K. Denis, X. Sun, J. Zhang, L. Hou, X. Zhang and C. Yuan, *Electrochim. Acta*, 2019, **307**, 20–29.
33 S. Rengaraj, S. Venkataraj, S. H. Jee, Y. Kim, C. Tai, E. Repo, A. Koistinen, A. Ferancova and M. Sillanpaa, *Langmuir*, 2011, **27**, 352–358.
34 L. Wang, F. Tang, K. Ozawa, Z. Chen, A. Mukherj, Y. Zhu, J. Zou, H. Cheng and G. Q. Lu, *Angew. Chem., Int. Ed.*, 2009, **48**, 7048–7051.
35 L. Wang, Y. Sun, S. Zeng, C. Cui, H. Li, S. Xu and H. Wang, *CrystEngComm*, 2016, **18**, 8072–8079.
36 Y. Mu, L. Wang, Y. Zhao, M. Liu, W. Zhang, J. Wu, X. Lai, G. Fan, J. Bi and D. Gao, *Electrochim. Acta*, 2017, **251**, 119–128.
37 K. O. Moura, R. J. S. Lima, A. A. Coelho, E. A. Souza-Junior, J. G. S. Duque and C. T. Meneses, *Nanoscale*, 2014, **6**, 352–357.
38 Z. Fu, J. Hu, W. Hu, S. Yang and Y. Luo, *Appl. Surf. Sci.*, 2018, **441**, 1048–1056.
39 Z. Jin, C. Liu, K. Qi and X. Cui, *Sci. Rep.*, 2017, **7**, 39695.
40 B. Malik, K. Vijaya Sankar, R. Konar, Y. Tsur and G. D. Nessim, *ChemElectroChem*, 2021, **8**, 517–523.

41 K. C. Majhi, P. Karfa, S. De and R. Madhuri, in IOP Conference Series: Materials Science and Engineering, IOP Publishing, 2019, vol. 577, p. 12076.
42 M. Shen, C. Ruan, Y. Chen, C. Jiang, K. Ai and L. Lu, *ACS Appl. Mater. Interfaces*, 2015, **7**, 1207–1218.
43 Y. Wang, Y. Zhang, Z. Liu, C. Xie, S. Feng, D. Liu, M. Shao and S. Wang, *Angew. Chem., Int. Ed.*, 2017, **56**, 5867–5871.
44 B.-A. Mei, O. Munteshari, J. Lau, B. Dunn and L. Pilon, *J. Phys. Chem. C*, 2018, **122**, 194–206.
45 F.-T. Tsai, Y.-T. Deng, C.-W. Pao, J.-L. Chen, J.-F. Lee, K.-T. Lai and W.-F. Liaw, *J. Mater. Chem. A*, 2020, **8**, 9939–9950.
46 P. T. Babar, A. C. Lokhande, M. G. Gang, B. S. Pawar, S. M. Pawar and J. H. Kim, *J. Ind. Eng. Chem.*, 2018, **60**, 493–497.